The Role of Salt Tectonics, Glacioeustatic Variations, and High pH Evaporitic Groundwater in the Development of Synsedimentary Paleokarst within Carboniferous Polymictic Fanglomerate at Hopewell Cape, Atlantic Canada

*Pierre Jutras**

Department of Geology, Saint Mary's University, Halifax, Nova Scotia B3H 3C3, Canada

ABSTRACT

A succession of Lower Carboniferous polymictic conglomerate in eastern Canada is truncated by synsedimentary endokarst conduits, which are clogged by lithified karst infill. Although such rocks do not usually host karst because of their polymineralic and poorly soluble contents, there are contextual and geochemical lines of evidence suggesting that groundwater conditions may have been highly alkaline at the time of karst formation, thus substantially increasing the solubility of common silicate minerals. The succession was deposited in a hyperarid climate and in close proximity to an evaporitic marine body. Because of a combination of high subsidence rates along a basin-bounding normal fault and entrapment within a salt expulsion minibasin, the evaporitic body of water was forced to prograde toward the source area of the sedimentary basin. This restricted sea was also responding to ongoing glacioeustatic variations at the time, which are interpreted to have generated a cyclic progradation of evaporitic groundwater into basin margin fanglomerates, thus favoring their early cementation by calcite. Karstification of the siliciclastic material is interpreted to have occurred during cyclic retreats toward lowstands, when groundwater alkalinity may have been highest.

Introduction

Karst is unlikely to develop in poorly soluble rocks, especially those that are not nearly monomineralic in composition, because solubility conditions tend to be mineral specific in the range of natural environments, and insoluble impurities tend to clog the karst system early in its development (Ford and Williams 2007). In rare cases in which caves are found in such rocks, the processes involved are usually dominated by weathering and ablation processes rather than congruent solution, and in such cases, the resulting caves are therefore referred to as pseudokarst (e.g., Jordan and Jones 2005; Vidal-Romani and Vaquiero-Rodriguez 2007). However, Willems et al. (2002) provided evidence for the development of dissolution caves (i.e., pure karst) in granite of South Cameroon under extremely acidic groundwater conditions on the basis of the presence of taranakite in speleothems, which precipitates only at a pH below 3.5. At such low pH, most crustal rocks should theoretically undergo nearly congruent solution, because even the most stable residual products of rock weathering—such as gibbsite, hematite, and goethite—are relatively soluble under a pH of 3.5 (Blatt et al. 1980), which occurs only rarely in natural environments. I here provide evidence for the development of multimetric synsedimentary karst in polymicticic conglomerate of the Visean (Lower Carboniferous) Hopewell Cape Formation at Hopewell Cape, New Brunswick, Canada (fig. 1), which evolved in a hyperarid climate (Jutras et al. 2015) that was very unlikely to develop low pH conditions but which may have developed equally aggressive high pH groundwater. In this article, field relationships are described and discussed first to better orient the geochemical study of the karst infill.

Manuscript received August 5, 2015; accepted March 5, 2016; electronically published June 20, 2016.

* E-mail: pierre.jutras@smu.ca.

Geological Setting

The Brigantian (uppermost Visean) Hopewell Cape Formation of Ami (1902; revised by St. Peter and Johnson 2009) was assigned to the Mabou Group of

[The Journal of Geology, 2016, volume 124, p. 447–462] © 2016 by The University of Chicago. All rights reserved. 0022-1376/2016/12404-0002$15.00. DOI: 10.1086/686630

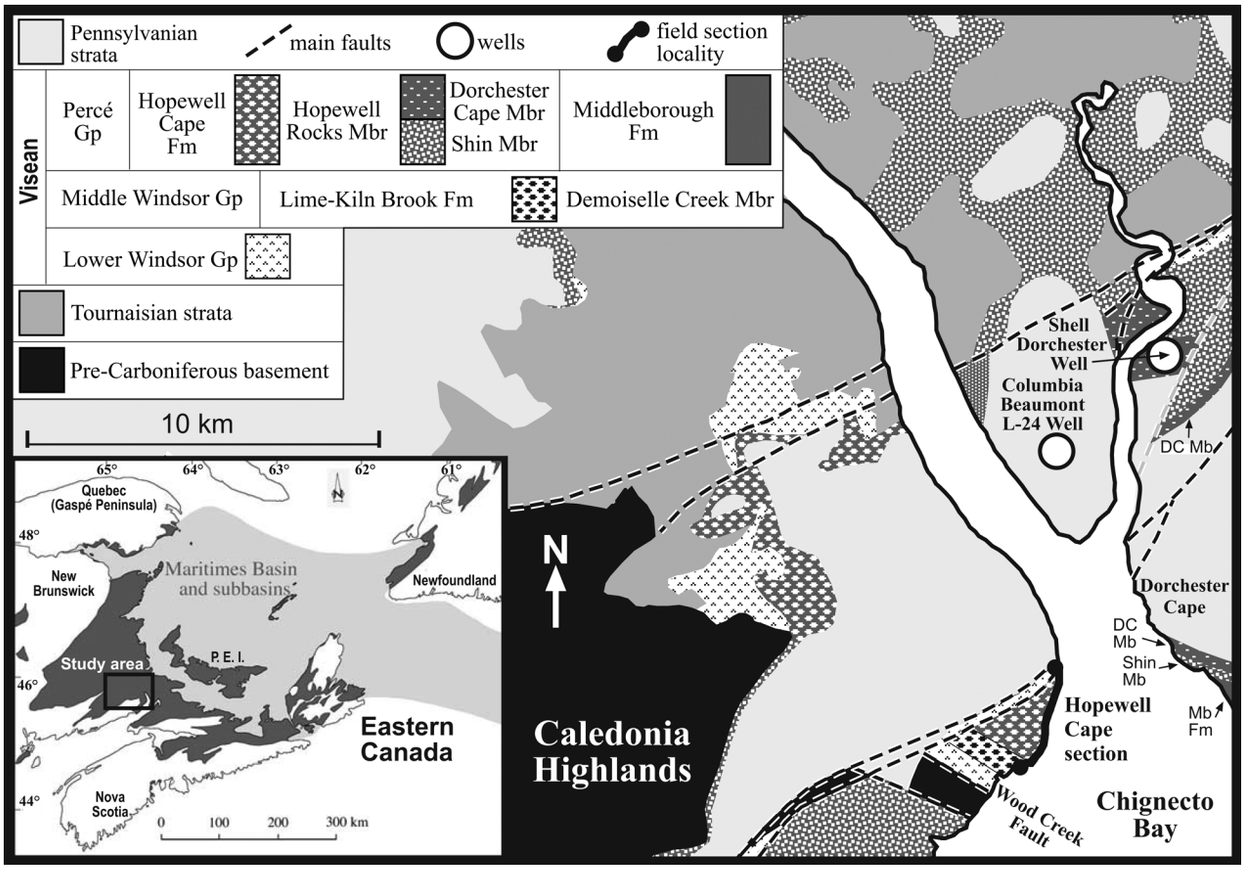

Figure 1. Geology of the study area (after St. Peter and Johnson 2009; Jutras et al. 2015).

Belt (1964) by St. Peter and Johnson (2009) and more recently assigned to the continental Percé Group of Jutras and Prichonnet (2005) by Jutras et al. (2015; fig. 2). At Hopewell Cape, in the western portion of the late Paleozoic Cumberland Basin of New Brunswick and Nova Scotia (fig. 1), this formation is characterized by its Hopewell Rocks Member, a thick succession of planar-bedded pebble to cobble conglomerate (Jutras et al. 2015; fig. 2). This member conformably overlies the upper Asbian (upper Visean) Demoiselle Creek Member (McCutcheon 1981; revised by Jutras et al. 2015) of the Lime-Kiln Brook Formation of Ryan and Boehner (1994), which is characterized by alternations of marine limestone with similar conglomerate (fig. 3*A*), and which belongs to the Middle Windsor Group (sensu Giles 1981; fig. 2). According to correlations with regional wells, the Lime-Kiln Brook Formation and most (if not all) of the overlying Hopewell Rocks Member transition laterally into calcium sulphate of the Dorchester Formation (Jutras et al. 2015; fig. 4), which also belongs to the Middle Windsor Group (fig. 2). The latter subgroup unconformably overlies the Lower Windsor Group, which—above a thin base of carbonate rocks—is characterized by a few hundred meters of mid-Visean sulphate and a layer of salt that is estimated to have been ~2–3 km thick before subsequent diapirism in the Cumberland Basin (Waldron et al. 2013).

On the basis of seismic (Waldron et al. 2013) and sedimentological (Jutras et al. 2015) evidence, expulsion of the Lower Windsor Group salt was already ongoing in the Cumberland Basin in upper Asbian times, influencing sedimentation for the remainder of the Carboniferous. In the study area, the Shell Dorchester 1 well includes nearly 1 km of salt (part of the Dorchester Dome of Martel 1987) separating Lower Windsor sulphate from Middle Windsor sulphate, whereas none is found ~4 km to the southwest in the Columbia Beaumont L-24 well (fig. 4). The sulphate interval in the latter well is therefore interpreted as combined Lower and Middle Windsor Group sulphates separated only by a salt weld that is also recognized in the local field geology,

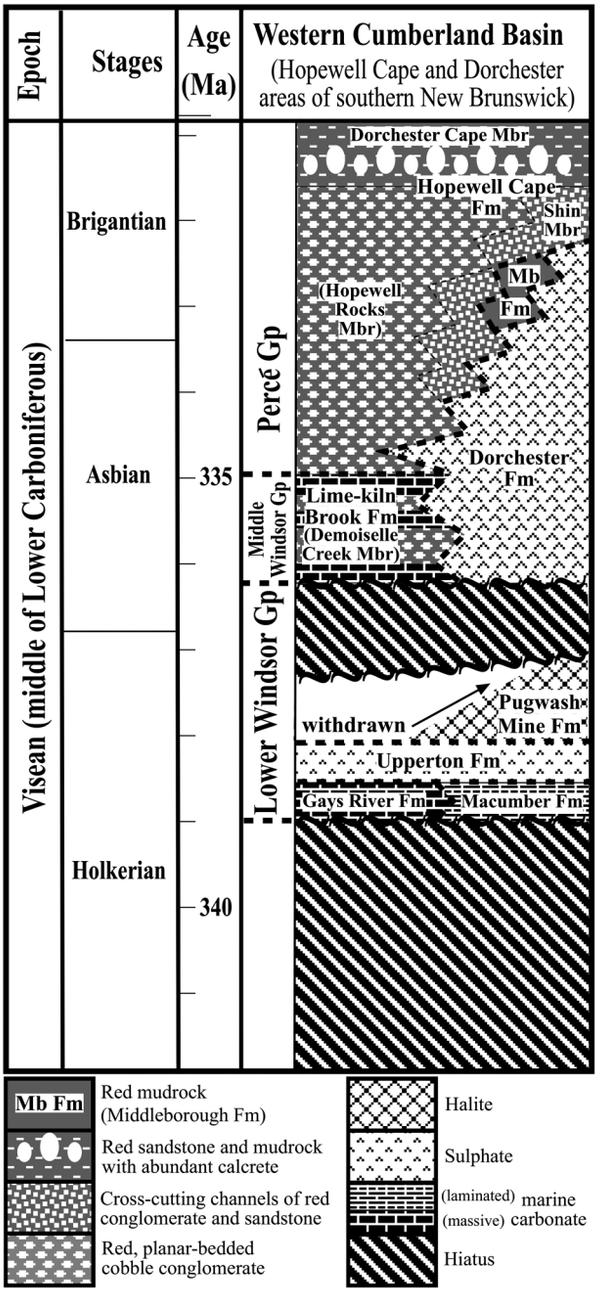

Figure 2. Visean stratigraphy of the study area (after St. Peter and Johnson 2009; Jutras et al. 2015). Time scale after Richards (2013).

~5 km to the north, where Percé Group rocks directly lie on Tournaisian strata with no intervening Windsor Group strata (Jutras et al. 2015).

Petrography and Sedimentology of the Karst-Hosting Polymictic Conglomerate Succession

The ~530-m section that hosts karstic features at Hopewell Cape was studied in detail by Jutras et al. (2015) and is only summarized here. Most of the section is characterized by a monotonous, planar-bedded succession of red, polymictic, pebble to cobble conglomerate (fig. 3*A*), which was sourced from the nearby Caledonia Highlands and sharply separated from them by the Wood Creek Fault scarp (Jutras et al. 2015; fig. 5). The conglomerates are poorly rounded, poorly sorted, and matrix to clast supported but are mud poor and show clear evidence of vertical

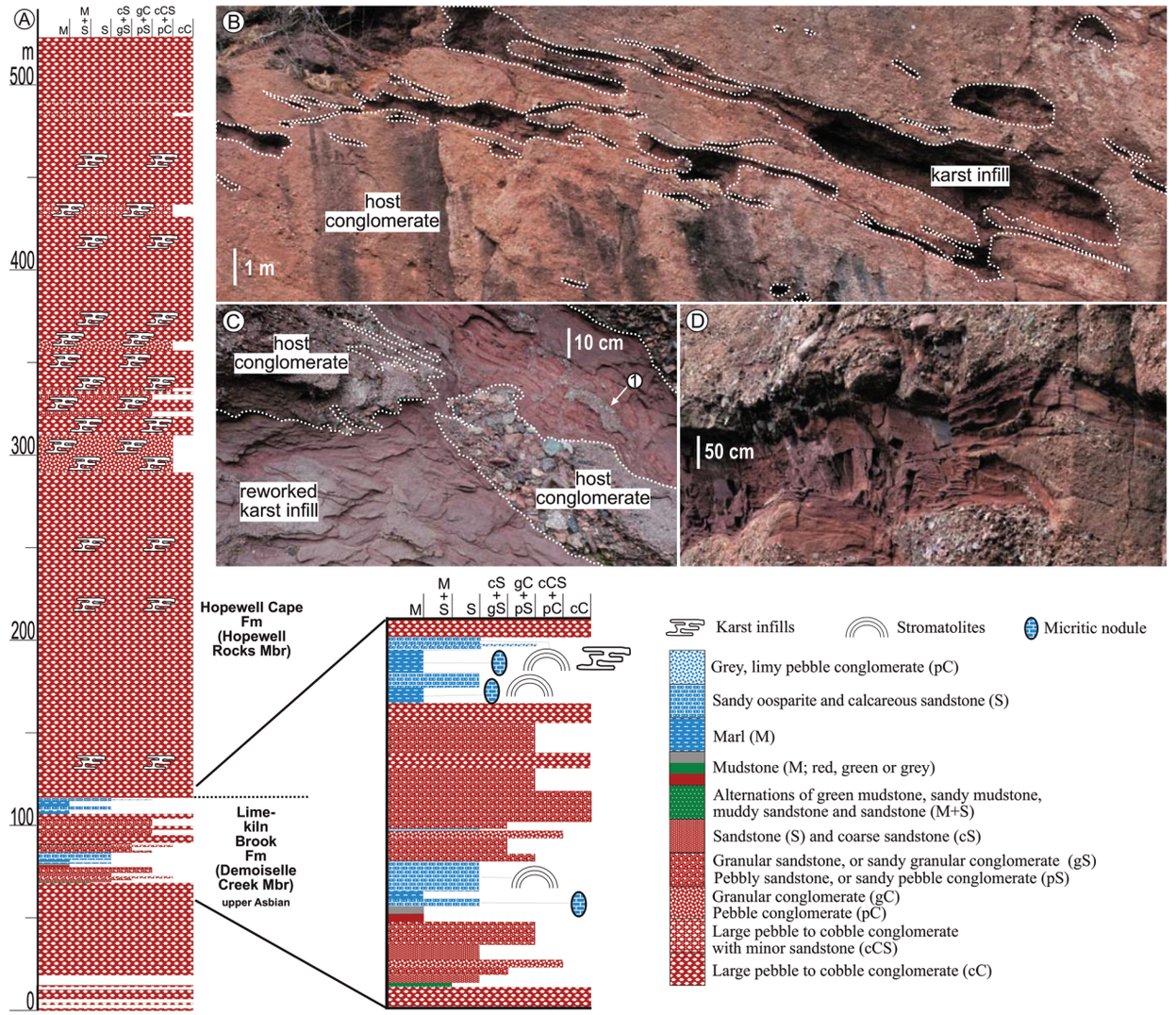

Figure 3. *A*, Hopewell Cape section in southern New Brunswick. *B*, General view of sediment-filled endokarst conduits that truncate the Visean conglomerates of the Hopewell Rocks Member at Hopewell Cape. *C*, Second-generation muddy karst infill (pockets of darker red material) in the vicinity of a small vertical shaft; the material labeled as 1 is a small example of ceiling failure (i.e., the collapse of host conglomerate into karst infill material). *D*, Thin remnants of host conglomerate pinching out into karst infill material at the edge of a large endokarst conduit.

aggradation. They are therefore interpreted as flash flood deposits (Jutras et al. 2015). Because of the planar nature of the coarse conglomeratic facies, which suggests high base level, and because of its occasional interbedding with marine carbonate rocks, the succession is interpreted as belonging to a fan delta setting (Jutras et al. 2015).

The last occurrence of carbonate rocks marks the transition between the Lime-kiln Brook Formation (Middle Windsor Group) and the overlying Hopewell Cape Formation (Percé Group), which—although incomplete—is four times thicker at Hopewell Cape than in the nearby Dorchester Cape section, just across Chignecto Bay (Jutras et al. 2015; fig. 1). To explain these greater sedimentation rates at Hopewell Cape, Jutras et al. (2015) suggested that exceptionally high basin subsidence rates were occurring at that locality because of ongoing salt expulsion paired with rapid movement along a basin-bounding normal fault (fig. 5).

Restricted marine conditions during deposition of the Lime-kiln Brook Formation at Hopewell Cape

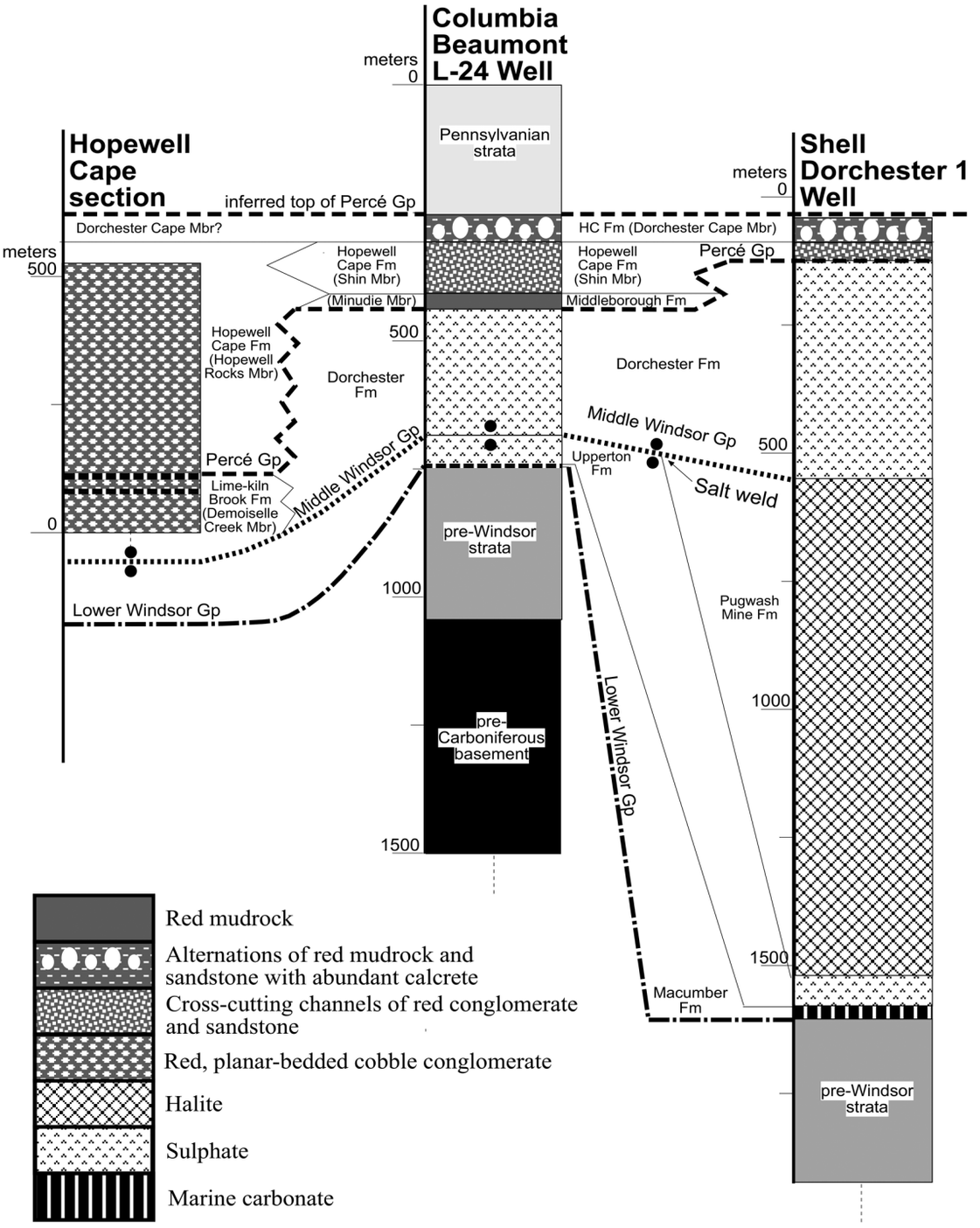

Figure 4. Correlations between the Hopewell Cape section and nearby wells in the area of the Dorchester Salt Dome (localities are shown in fig. 1).

are suggested by stratigraphic data from nearby wells, which indicate that the fan delta conglomerates and carbonates of this unit and possibly all of the overlying Hopewell Rocks Member transition laterally into nearly continuous calcium sulphate (figs. 2, 4). This suggests that—except in the vicinity of the source area, where freshwater inputs were locally diluting the brines—the marine basin was otherwise too hypersaline for carbonates to be deposited (Jutras et al. 2015).

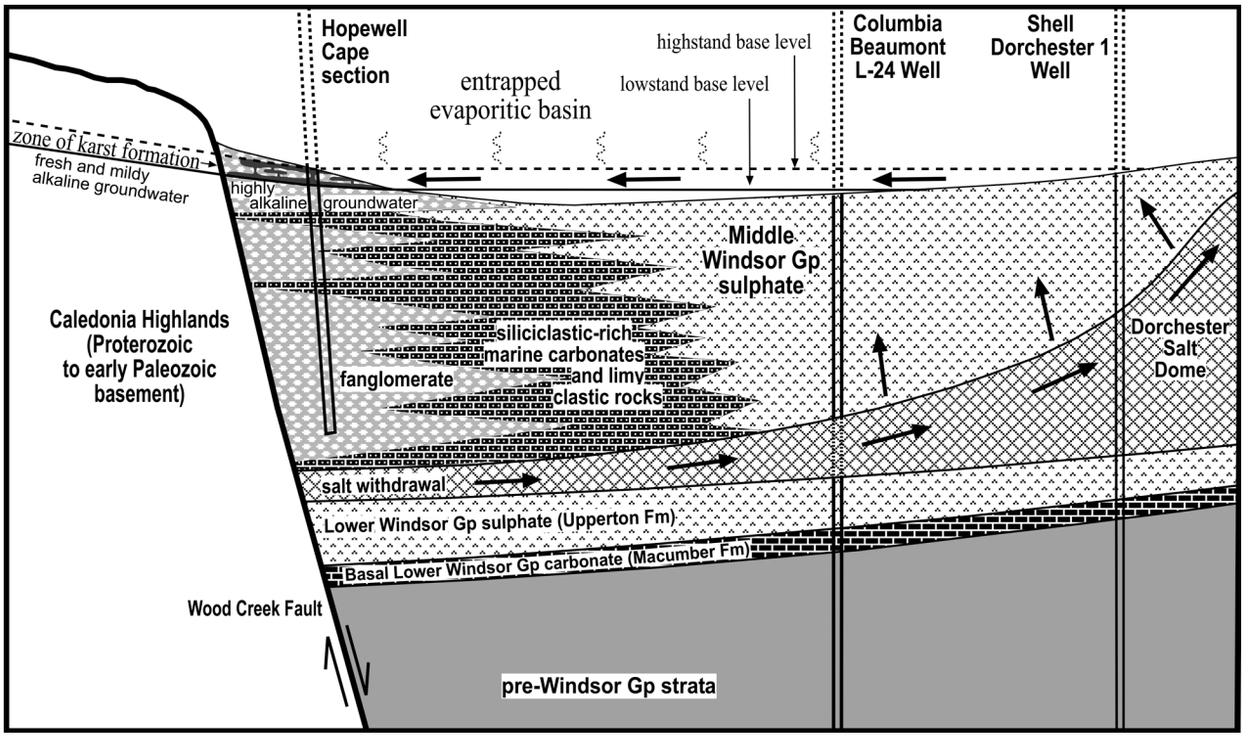

Figure 5. Model for the formation of karst in the proximal siliciclastic fanglomerate at Hopewell Cape through the cyclic progradation of highly alkaline evaporitic water. This progradation is inferred to have been caused by a combination of high subsidence rates along a basin-bounding normal fault, ongoing salt expulsion, and glacioeustatic highs.

Although nearby basins in eastern Canada were marked by well-defined sedimentary cycles controlled by glacioeustatic variations during the late Visean (Giles 2009), such clear sedimentary cyclicity is lacking in the Cumberland Basin, which Jutras et al. (2015) attributed to the long-term entrapment of marine bodies in salt expulsion minibasins. In the case of the minibasin in which the Hopewell Cape section was deposited, the lack of lateral continuity in the carbonate intervals, which all transition laterally into sulphate (fig. 4), suggests that this entrapped marine body may have been cut off from significant marine influxes (Jutras et al. 2015). However, even in this highly restricted context, it is expected that global glacioeustatic variations would still have resulted in base-level fluctuations in and around the minibasin.

Clast content in the Hopewell Rocks Member is quite consistent throughout the thick succession and is characterized by ~50% metamudrock (phyllite, slate, and minor schist), ~25% granite and felsic volcanics, ~20% quartzitic material (metaquartzite, metasiltstone, chert, and vein quartz), ~3% limestone, and ~2% metabasalt. This clastic material is cemented by goethite and spar (~3% and ~2%, respectively, of the volume on thin sections).

Karst Morphology and Karst Infill Petrography

Despite their siliciclastic petrography, the coarse conglomerates of the Hopewell Rocks Member are sharply truncated by endokarst conduits at Hopewell Cape, which are best developed in the middle of the exposed succession (fig. 3*A*) and which are up to 1.5 m thick and up to 15 m wide on outcrop (fig. 3*B*). They form distinct tunnels that stretch parallel to bedding and that are interconnected by a few short, perpendicular to bedding shafts (fig. 3*B*, 3*C*). The host conglomerate shows structural integrity around the cavities (fig. 3*B*–3*E*), indicating that the host material was well indurated before karst formation, which was a prerequisite for karst to be able to form and which precludes any soft sediment deformation processes to explain the truncations.

Upper contacts between the cavities and the host rock are always quite sharp and feature some dis-

solution rills. The lower contact is gradational in a few cases but mostly sharp and downcutting into the host material, sometimes reaching into a shaft that connects with an underlying gallery (fig. 3*B*, 3*E*). Side walls can be sharp and smooth (e.g., right side wall of the largest conduit of fig. 3*B*), but they can also be characterized by long and thin wedges of host conglomerate protruding into karst infill (e.g., fig. 3*D*; left side wall of the largest conduit of fig. 3*B*). In some instances, relatively large chunks of host conglomerate can be found within fine-grained karst infill (e.g., 1 in fig. 3*C*) and are interpreted as ceiling failure material. Also noteworthy is the observation that the smallest cavities (centimetric scale) are concentrated in rare and thin (less than 25 cm thick) sand-rich intervals (fig. 6).

Just as their floor and ceiling, bedding of the lithified karst infills is for the most part parallel to host rock bedding (fig. 3*B*). The exposed and accessible components of the red clastic infill material are characterized by ~5% granular to pebble conglomerate (mostly in the form of thin gravel lags with a similar clast composition as the host conglomerate), ~20% sandstone, and ~75% silty mudstone. In association with the only vertical shaft that is available for close observation, it also includes small pockets of claystone that are truncating the coarser karst infill material (fig. 3*C*).

Discussion on the Physical Evolution of the Karstic System

On the basis of field observations in areas where karst did not fully develop, it can be inferred that the karst system was first developing between bedding planes in more sandy intervals of the conglomeratic succession (fig. 6) and then expanded into the coarser material that dominates the succession (fig. 7). In a few conduits, the gradational lower contact of the karst infill suggests that formation of such discrete embryonic conduits did not always occur and that, in some areas where porosity was

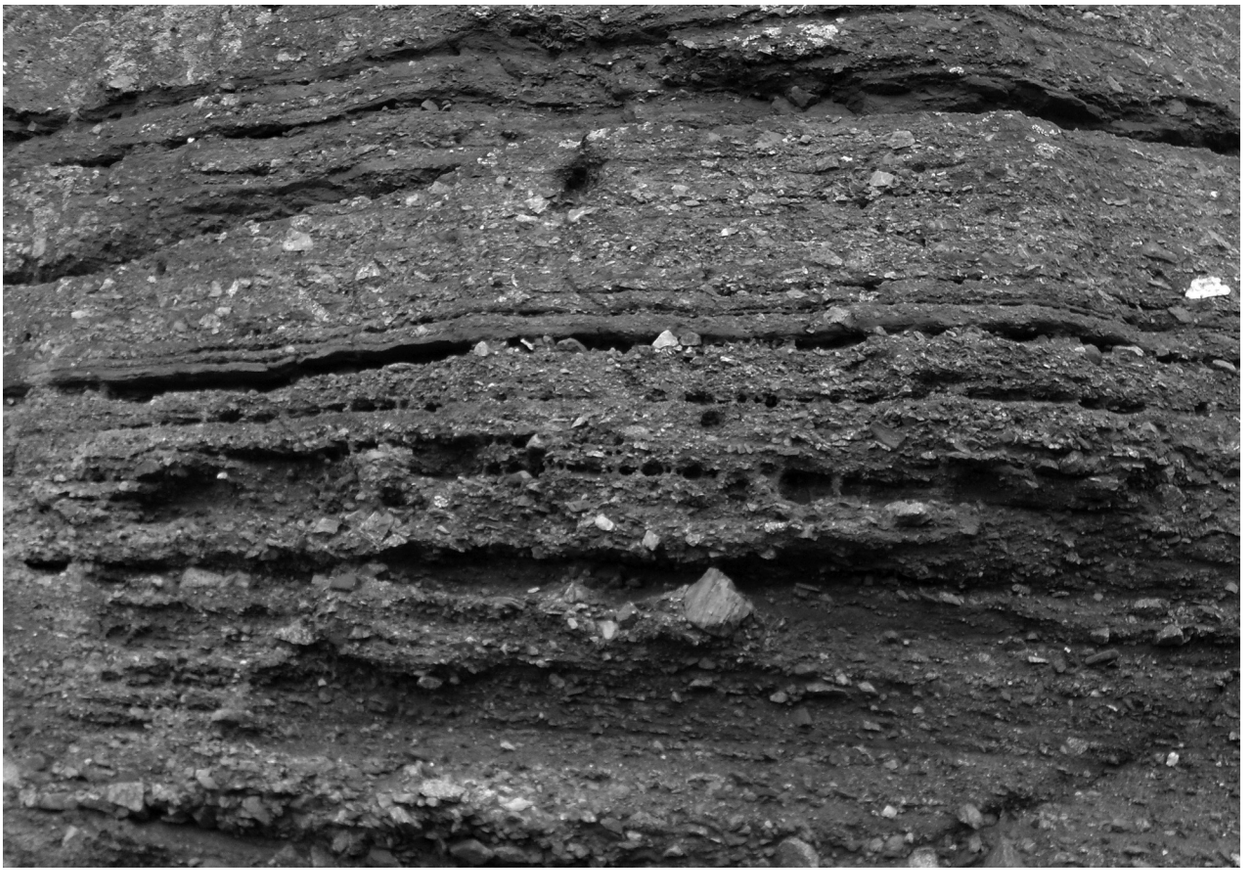

Figure 6. Small mudstone-infilled karstic conduits developed in thin sand-rich intervals of the coarse conglomeratic succession.

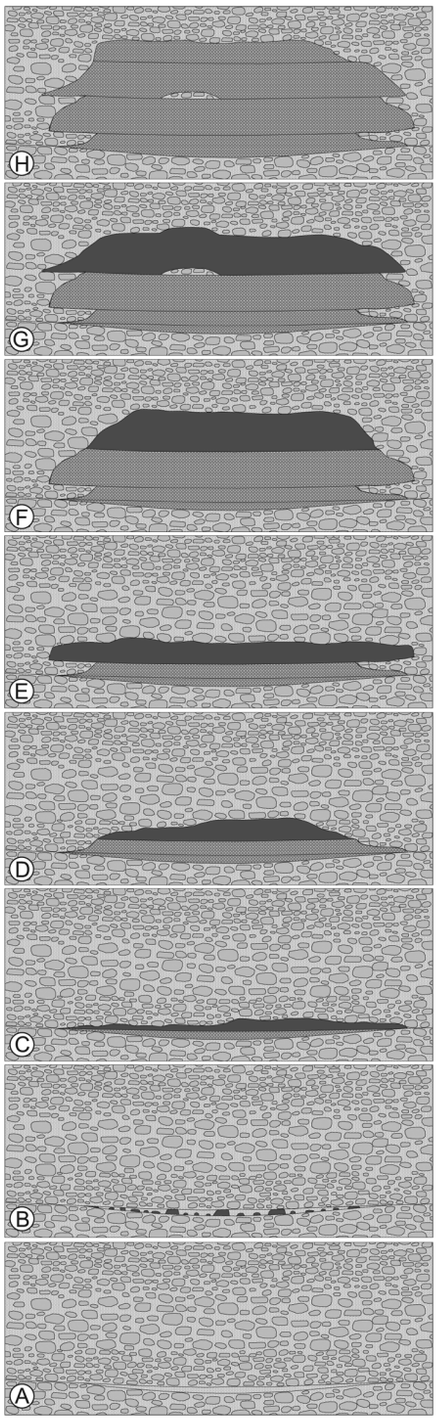

Figure 7. Model for the physical evolution of the karstic system based on field observations. A color version of this figure is available online.

especially well developed in the host material, diffuse intergranular flow could have occurred in early stages of karst formation, followed by an upward expansion of the karst system through the work of a more concentrated flow.

The lack of a concentration of collapse breccia or gravel lag at the lower contact with the host rock and their distribution at different levels of the karst infills suggest that the voids were never more than a few tens of centimeters in height and that periods of dissolution were alternating with periods of infilling (fig. 7). Remnants of in situ host material protruding deeply into karst infill at the edges of some of the larger karst structures (fig. 3*B*, 3*D*) are also best explained in the context of regularly alternating periods of dissolution and infilling, in which the width of the cavity may have varied greatly from one episode of dissolution to the next (fig. 7). As the conduit expanded in width, the more restricted cavity beneath would be anchored in karst infill and preserved as a narrower neck. In this view, the short vertical shafts are possibly formed by the same process but as especially narrow conduits. A tentative interpretation of successive cavity geometries is presented as timelines in figure 8.

The hypothesis of a thin, concentrated groundwater flow that gradually migrated upward in the succession implies relatively fast subsidence rates, which are inferred for this succession (Jutras et al. 2015). An alternative process would be that of a gradual merging of originally thin and discrete dissolution pathways in which groundwater flow was originally split vertically. We believe that the stratigraphy of the karst infills is insufficiently complex and that the lenticular remnants of host material that they include are too few to support the latter view. The sharp truncation of sandy or silty karst infill material by second-generation muddy karst infill (fig. 3*C*) indicates that some of the early karst infill was reworked by subsequent events of dissolution and infilling, possibly in association with an occasional slowdown of subsidence rates.

Timing of Karst Formation and Source of Karst Infill

Because the paleokarst tunnels at Hopewell Cape are parallel or nearly parallel to bedding and are not constrained by sharp lithological boundaries, their geometry is most likely controlled by the position of the water table at the time of their formation, which suggests that they must have developed before the 35° tilting of the succession. Their sporadic distribution along several hundred meters of section suggests that they developed during shallow burial, when the Visean basin was still actively receiving sediments, and that they are the record

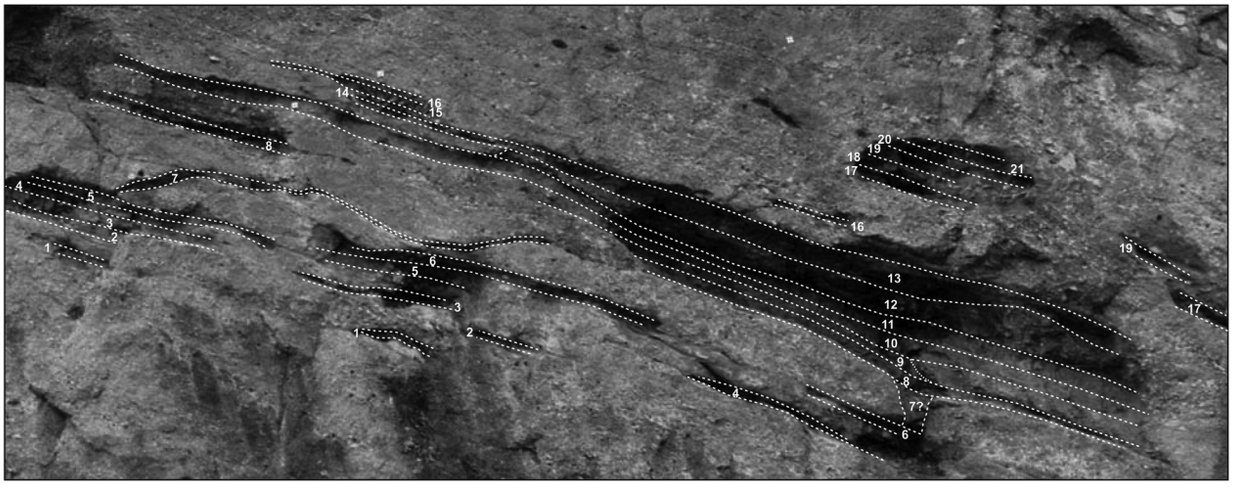

Figure 8. Example of tentative timelines in the development of the karst system by alternating phases of dissolution and deposition (each timeline represents one cycle) and by upward migration in association with basin subsidence. A color version of this figure is available online.

of groundwater circulation at successive water table levels.

Geochemistry and Mineralogy of the Karst Infills and Their Host Rock

The synsedimentary nature of the karst implies that, although the karst infill might include material derived from outside the system by infiltration into the cavities, this material would have been from the same source as its host conglomerate and in the same environment. Any significant changes in chemical and mineralogical compositions from host rock to karst infill can therefore be attributed to processes having occurred within the karst system. Although the karst infills must be the record of lull periods when groundwater conditions were not aggressive enough to cause significant dissolution in the karst system, they show evidence of having been periodically reworked by karst processes and can therefore provide clues regarding karst water chemistry.

Analytical Methods. The mineralogical and geochemical compositions of karst infills are here compared with their conglomeratic host rock on the basis of the X-ray fluorescence and X-ray diffraction analyses of powdered field samples (table 1). Eight large samples (>1 kg) of conglomeratic host rock distributed from the base of the studied karst infills to 100 m above were crushed and pulverized for analysis, as well as six samples of silty mudstone and three samples of claystone in the karst infills. Although the claystone component is a key element for understanding the paleo-groundwater chemistry of the karstic system, it is exceedingly rare in the accessible parts of the system, hence its limited sampling.

X-ray fluorescence analyses were performed at the Regional Geochemical Centre of Saint Mary's University (Halifax, Nova Scotia), using a Phillips PW2400 X-ray spectrometer. Major element concentrations were determined using the fusion method on glass disks, whereas trace elements were analyzed separately using pressed pellets from the same powdered sample.

X-ray diffraction analyses for all samples were performed on a Siemens D5000 diffractometer hosted at the Département des Sciences de la Terre et de l'Atmosphère de l'Université du Québec à Montréal, Canada, and one of the silty mudstone sample (sample J-02-04) was additionally studied with scanning electron microscopy (SEM) and energy-dispersive spectroscopy (EDS) element mapping (Oxford Instruments LEO 1450 VL) at the Regional Geochemical Centre of Saint Mary's University.

Results and Discussion. Our results show that the geochemical composition of the conglomerate is relatively well constrained in the ~100 m of studied section, apart from Ca, which varies along with the amount of calcite cement (fig. 9). This corroborates the observed petrographic monotony of the thick conglomeratic succession, which does not vary much in terms of clast contents. However, clear variations in composition can be observed from host rock to karst infill (fig. 9), some of which may be explained by sorting processes. For example, because Zr tends to concentrate in silt-size zircons, it is strongly enriched in the silty mudstone fraction but depleted in

Table 1. X-ray Fluorescence (XRF) Analyses (%)

XRF data	SiO_2	TiO_2	Al_2O_3	Fe_2O_3	MnO	MgO	CaO	Na_2O	K_2O	P_2O_5	LOI	Sum
Conglomerate host rock:												
J-12-01	66.0	.5	12.7	4.0	.1	1.8	4.4	3.3	1.9	.1	5.2	99.9
J-13-14	68.2	.6	13.5	5.1	.1	2.2	2.4	3.3	2.1	.1	2.0	99.7
J-13-11	66.1	.6	13.5	5.2	.1	2.2	4.2	3.4	2.0	.2	2.8	100.2
J-13-12	65.4	.6	13.2	5.3	.1	2.5	4.6	3.1	1.7	.1	3.4	100.0
J-13-13	63.1	.8	14.8	6.7	.1	2.6	3.4	3.4	1.7	.2	2.9	99.6
J-13-15	68.9	.6	13.7	4.9	.1	2.0	2.5	3.4	2.0	.1	2.0	100.1
J-13-16	63.5	.6	12.9	4.6	.1	2.2	6.6	3.2	1.9	.1	4.6	100.4
J-13-17	63.3	.6	12.5	4.7	.1	2.5	5.8	2.8	1.8	.1	4.6	98.7
Silty mudstone karst infill:												
J-12-04	66.6	.8	10.7	5.8	.1	2.7	3.2	1.5	2.2	.1	5.5	99.2
J-13-01	67.7	.8	10.4	5.4	.1	3.0	3.2	1.7	2.3	.2	4.9	99.6
J-13-4	69.9	.9	10.5	6.0	.1	2.8	2.2	1.3	2.4	.1	3.9	100.0
J-13-5	65.8	.9	12.3	6.7	.1	3.5	2.6	1.9	2.4	.2	4.0	100.2
J-13-6	68.1	.8	11.1	5.6	.1	3.0	2.9	1.5	2.6	.1	4.6	100.3
J-13-7	66.8	.7	10.8	5.5	.1	2.8	4.0	1.7	2.4	.1	5.3	100.3
Claystone karst infill:												
J-12-05	57.6	.8	14.5	8.9	.1	4.2	2.1	1.2	3.4	.1	6.5	99.3
J-13-02	51.5	.8	17.6	12.4	.1	5.0	1.4	.8	4.6	.1	6.0	100.3
J-13-3	59.6	.8	14.4	8.5	.1	4.3	2.2	1.3	3.4	.1	5.7	100.3

Note. Data from glass disk. Detection limit is 0.1% for major elements (fusion method) and 1 ppm for minor elements (pressed-pellets method). Total values do not include trace elements. Detection limit is 0.1%. LOI = loss on ignition.

the claystone fraction relative to other relatively immobile elements, such as Y, Nb, and Ti (fig. 9).

Element concentrations that are least influenced by either sorting or dissolution are interpreted to be those who show a gradual increase from the host conglomerate to the finer end members of the karst infill, such as Y, Nb, Ti, Fe, K, and Mg (fig. 9). Of these, Nb shows the most constrained concentrations and is therefore used here as an inferred immobile element to assess mass gains and losses in other elements from conglomeratic host rock to karst infill by using the element mass transfer coefficient of Anderson et al. (2002; modified from Brimhall et al. 1992; fig. 10).

Our mass balance calculations indicate that the karst infill material is strongly depleted in Na, Ca, Mn, P, Si, and Al relative to Nb (fig. 10). Stronger depletion of Al and Mn in the silty mudstone fraction than in the claystone fraction (fig. 10) is interpreted as an artifact of sorting because these elements tend to concentrate in the clay or micaceous fraction during weathering. A similar deflection to the right from silty mudstone to claystone is observed in Fe, K, and Mg concentrations, which can also be attributed in part to sorting, but their distribution on each side of the Nb line (fig. 10) does not suggest any net loss by dissolution but rather suggests that they were as stable as Nb in the karstic system, although all the elements that are concentrated in the clay fraction (including Nb) may have experienced a certain degree of removal in suspension.

Our data also suggest that Fe, K, and Mg were possibly more stable than Y and Ti in the karstic system and significantly more stable than Si and Al (fig. 10), a substantial amount of which must have left the system entirely. Such immobility of K and Mg in near-surface weathering processes is very uncommon because they are usually easily removed in solution during the breakdown of primary minerals, whereas much of the Al typically tends to stay behind in secondary clay minerals. In our samples, the $Al_2O_3/(K_2O + MgO)$ ratio evolved from an average of 3.24 in the host rock to an average of 2.06 in the silty mudstone karst infill and 1.98 in the claystone karst infill (table 1).

The elements that show evidence of high mobility in the system (oxides of Si, Al, Ca, Na, Mn, and P; fig. 10) comprise on average 90% of the host rock volume along with volatiles (table 1). It can therefore be extrapolated that the host rock was undergoing nearly congruent solution, although variations in hydrologic conditions must have resulted in a cyclic alternation between phases during which the karst system was being infilled and partly clogged with residue and phases during which the karst system was expanding and residues were being reworked.

In terms of mineralogy, framework silicates vary only in terms of relative abundances from host rock to karst infill, but phyllosilicates vary also in terms of composition, being characterized by a variety of chlorites and metamorphic micas in the host conglomerate material but mostly Mg-rich chlorite (clinochlore),

Table 2. Semiquantitative X-ray Diffraction (XRD) Analyses (%)

XRD data	Quartz	Albite	K-feldspars	Muscovite + biotite	Phengite + sericite	Mixed chlorite	Clinochlore	Calcite	Dolomite	Hematite	Amorphous fraction
Conglomerate host rock:											
J-12-01	27	13	14	4		5		7	2		26
J-13-14	29	29	8		8	11				1	16
J-13-11	27	27	7		7	15		2		1	14
J-13-12	26	24	7		6	13		2		1	21
J-13-13	28	27	7		7	11		1			18
J-13-15	28	27	7		7	11		2			19
J-13-16	23	23	6		5	12		5	2		25
J-13-17	22	27	6		6	12		5	2		21
Silty mudstone karst infill:											
J-12-04	37	9	13		4		8	7	2	1	18
J-13-01	36	13	8	5	(+7% amphibole)		8	2	1	1	20
J-13-04	43	12	5	8			10	2	1	1	18
J-13-05	37	15	6	6			11	2		2	19
J-13-06	45	14	6	6			11	2		1	15
J-13-07	51	12	5	5			9	2	1	1	14
Claystone karst infill:											
J-12-05	33	7	6		6		9	9		1	28
J-13-02	28	16	7	11			13	2	1	2	19
J-13-03	33	14	5		9		11	2	1	1	24

Note. Data from rock powder. Analyses performed at the Département des Sciences de la Terre et de l'Atmosphère de l'Université du Québec à Montréal, Canada.

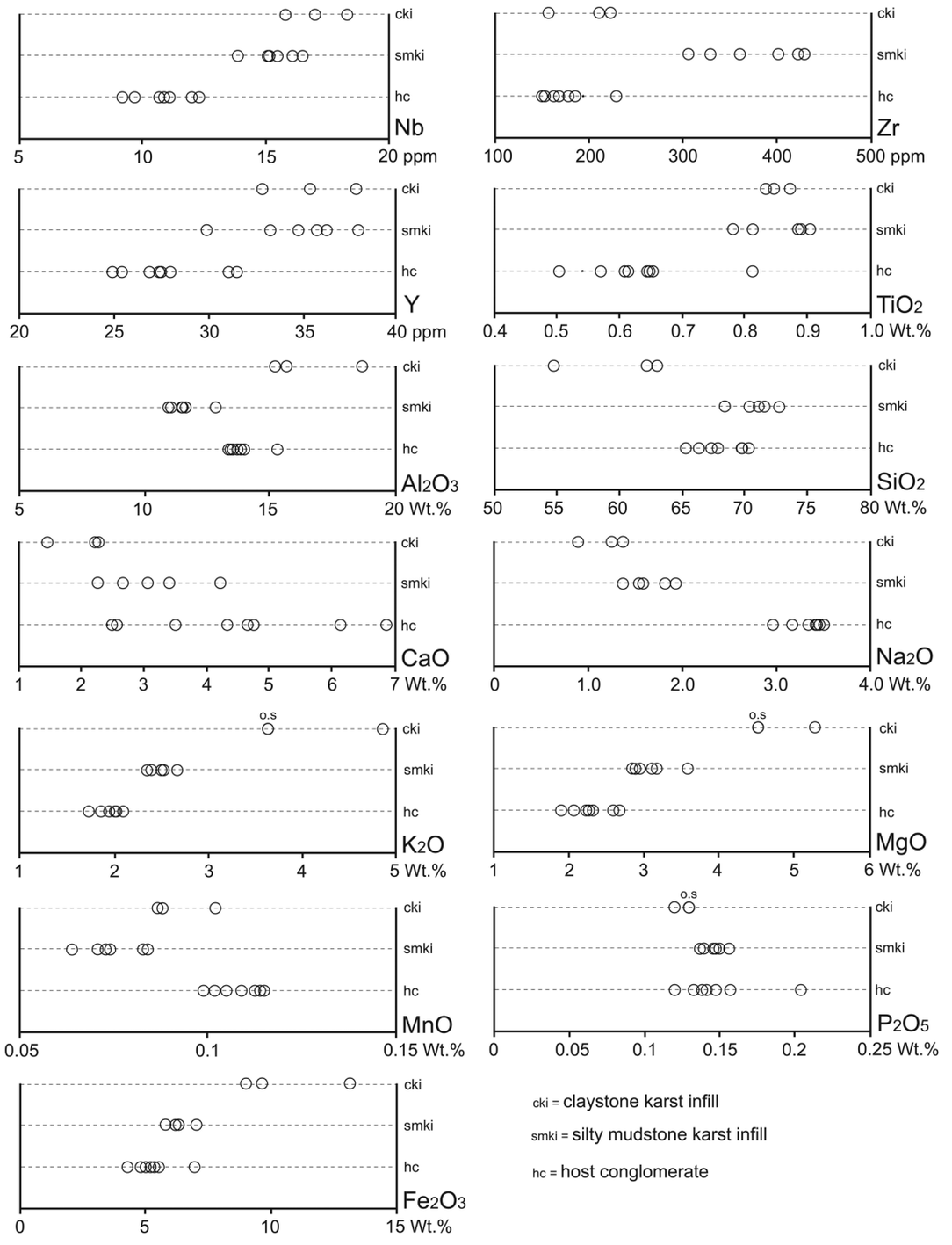

Figure 9. Concentration of major elements and selected trace elements in the host conglomerate (hc), silty mudstone karst infill (smki), and claystone karst infill (cki) on a loss on ignition–free basis (raw data in table 1).

muscovite, and biotite in the karst infill material (table 1). On the basis of SEM and EDS element mapping data, the original muddy matrix of the karst infill recrystallized during deep burial as tightly interstratified biotite, muscovite, and clinochlore, in which much of the K and Mg is now found (fig. 11*a*). Replacement of albite by muscovite is also commonly observed, but of particular interest is the replacement of albite by clinochlore (fig. 11*b*). The latter replacement is subsequent to deposition into the karst

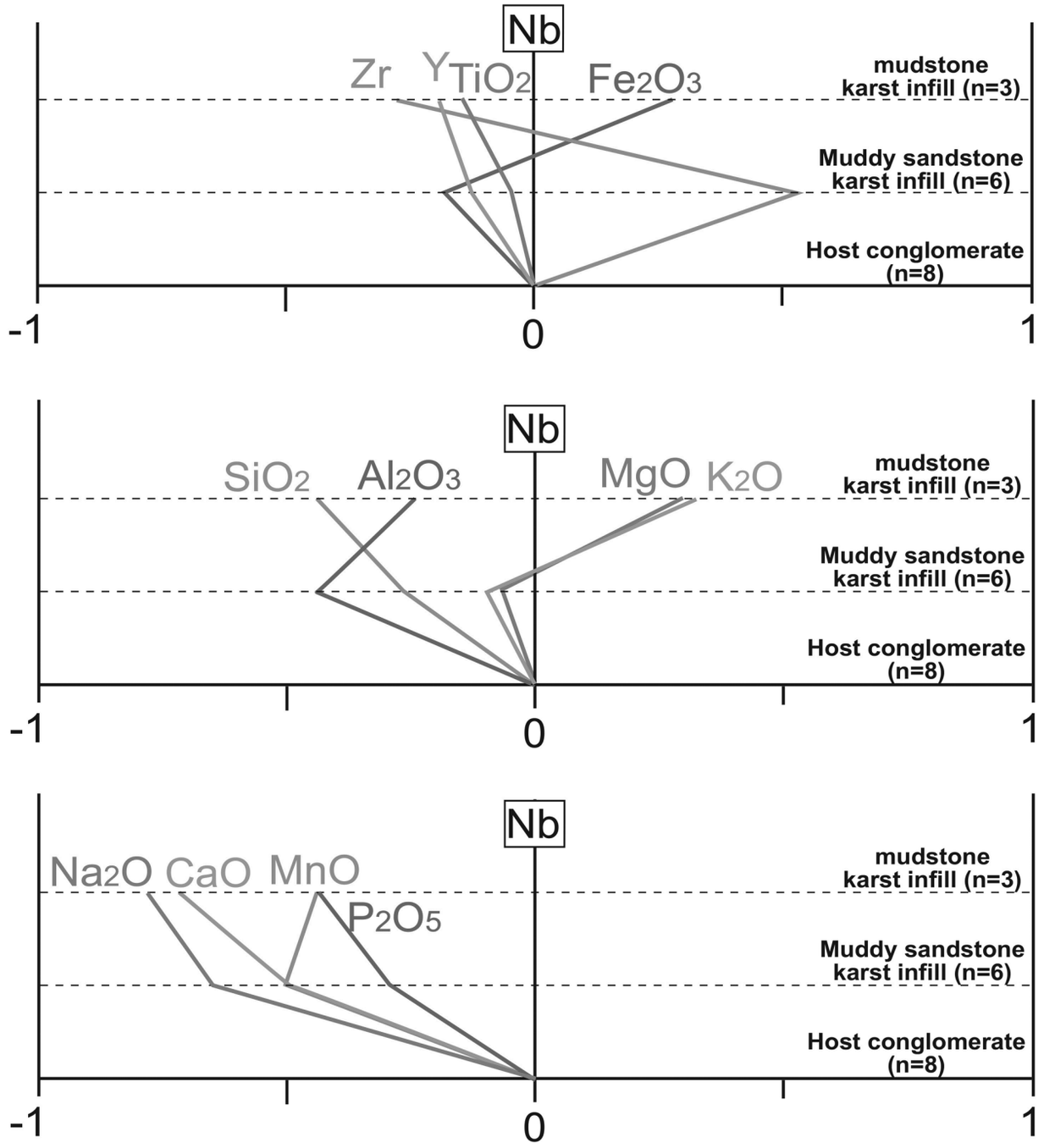

Figure 10. Elemental mass gains and losses from host rock to silty mudstone and claystone karst infill, based on the dimensionless element mass transfer coefficient of Anderson et al. (2002; modified from Brimhall et al. 1992), assuming Nb immobility. A color version of this figure is available online.

infill, since the altered grains would have been structurally too weak to remain intact during transport.

Paleokarst Water pH Assessment

As the Hopewell Rocks conglomerates are oxidized, barren in terms of visible organic matter and laterally transitioning into evaporites, they are interpreted as having evolved in a hyperarid environment (Jutras et al. 2015). Because they harbor an array of poorly soluble minerals, it is argued that synsedimentary karst could develop in them only under extreme groundwater pH conditions. It is also argued that in the arid environment that was

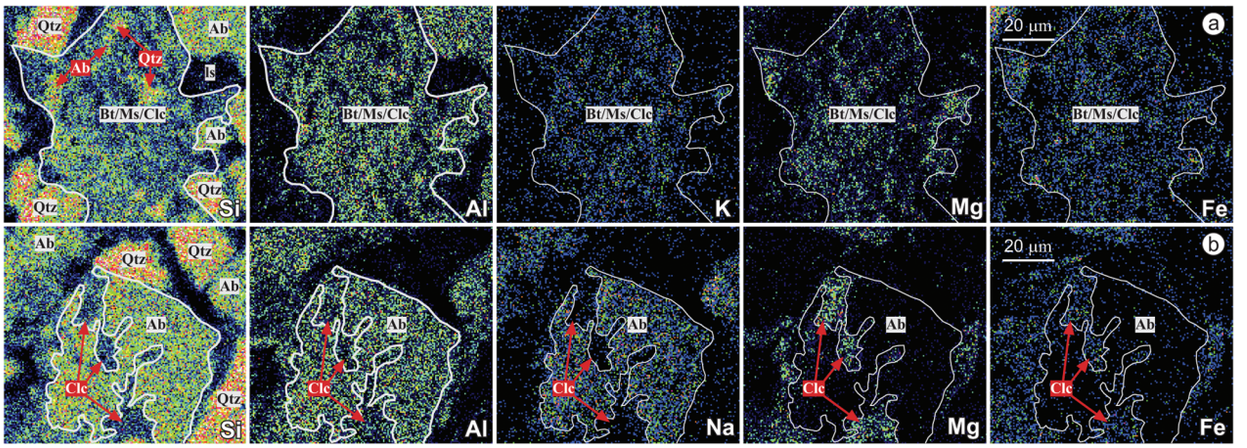

Figure 11. Energy-dispersive spectroscopy element mapping in karst infill material using a scanning electron microscope. *a*, Muddy matrix material recrystallized as interstratified biotite, muscovite, and clinochlore. *b*, Albite grain showing authigenic clinochlore replacement.

prevailing at the time, only a high pH range was achievable.

The lack of association between K or Mg concentrations and veining, zoning, or pore-filling cement on the EDS element maps does not suggest that significant inputs of these elements came from meso- or telodiagenetic fluids. The geochemical differences between karst infill and host rock are therefore interpreted as early diagenetic and directly related to karst processes. Because of the heterogeneous nature of the host rock, and because of the significant lateral displacement of material that may have taken place from host rock to karst infill, our estimations of elemental and mineralogical mobility are quite imprecise, but they do convincingly indicate that K and Mg were more stable than Si and Al (fig. 10), which corroborates the observation of a pervasive replacement of phyllosilicates and albite by K- and Mg-rich phases (fig. 11). The relative stability of K suggests that the karst system evolved under high pH conditions, and the incapacity of the system to remove Mg indicates that karst water pH must have been on average greater than 10.5, since this element evolves from being very soluble below a pH of 10 to virtually insoluble above a pH of 10.5 (Kvech and Edwards 2002). Studies on the solubility of high-Mg varieties of chlorite at low temperature and high pH are lacking in the literature, but a study by Azimov and Bushmin (2007) indicates that their solubility greatly decreases at high pH in metasomatic and metamorphic environments, and especially so for those with the highest Mg/Si ratios.

Although our assessment of mass balance variations from host rock to karst infill has inherent uncertainties related to transport, it can be argued that the pH of early diagenetic waters had to be in the alkaline range for clayish weathering products of any kind to harbour a lower $Al_2O_3/(K_2O + MgO)$ ratio than their host rock. The $Al_2O_3/(K_2O + MgO)$ ratio of 1.98 that is found in the claystone infill is in great contrast with the ratios that are typically found in the clay fraction of continental weathering products, which generally form in low pH conditions because of the ubiquitous presence of organic matter in environments that are humid enough to generate substantial weathering. In such settings, Al concentrations grow substantially at the expense of alkalis. For example, a Brazilian laterite developed in gneiss, a host that is similar to the Hopewell Rocks conglomerate in terms of bulk chemical composition, is reported to have an $Al_2O_3/(K_2O + MgO)$ ratio of 3530:1, as alkalis are nearly eradicated from soils in tropical humid environments (Schaefer et al. 2008).

Model for the Development of Karst by the Circulation of Alkaline Groundwater in the Hopewell Rocks Conglomerates

The development of synsedimentary karst implies that the clastic succession was cemented soon after deposition, thus forcing the phreatic flow to concentrate in discrete areas between aquitards. Early cementation by calcite and subsequent karst formation may have both been favored by a close connection of the fan to a restricted, hypersaline sea arm, which is indicated by a lateral transition from continental red beds to evaporites at that interval (fig. 4). Such restricted evaporitic water bodies tend

to develop very high pH values (Warren 2006), which can in turn greatly reduce calcite solubility and enhance the solubility of silicate minerals (Correns 1950; Blatt et al. 1980). Although evaporitic successions are typically regressive, progradation of the evaporitic basin toward the source area would have been favored by rapid movement along the basin-bounding normal fault and by ongoing salt expulsion into the Dorchester Salt Dome, which is known from wells located as close as ~10 km to the northwest (Jutras et al. 2015; figs. 1, 4). This tectonic and halokinetic setting would have effectively forced highly alkaline evaporitic seawater to invade the phreatic zone of the basin margin fanglomerate succession (fig. 5).

In early stages of minibasin development (the Lime-kiln Brook Formation interval), the entrapped marine body was abutting the source area during times of exceptionally high base level, which resulted in the interdigitation of marine carbonates among very proximal fanglomerates (figs. 3*A*, 5). In later stages (the Hopewell Rocks Member interval), the increasingly concentrated brines of the entrapped marine body would no longer reach the source area during highstands but may have come close enough for evaporitic groundwater to prograde into the proximal fanglomerates (fig. 5). This would also explain the unusually planar nature of this coarse fan succession, since a high water table would have favored rapid ground saturation and efficient lateral dispersion of surface runoff during heavy rainfall and associated flash flood deposition (Jutras et al. 2015). We interpret that early calcite cementation would have occurred during the progradation of evaporitic groundwater in times of rising base level and that karstification would have occurred during the gradual retreat of evaporitic groundwater toward lowstands (fig. 5), when groundwater pH may have been highest as a result of an accompanying decrease in marine influxes.

Whereas arid alluvial fans are typically dissected by a braided system of gullies between flash floods, during and following lesser events of rainfall, the fanglomerates at Hopewell Cape are not affected by substantial downcutting and channeling, which is possibly in part explained by the tight network of synsedimentary karst structures that is observed throughout the succession (fig. 3*A*). Minor events of discharge from the source area must have been quickly absorbed by the existing karst network, thus preventing downcutting.

Because dissolution of the siliciclastic conglomerates was not fully congruent, removal of a relatively large amount of residue must have occurred mechanically. According to Ford and Williams (2007), a high hydraulic gradient is necessary for caves to develop in rocks that include a high content of poorly soluble material so that the latter can be swept away by flowing water, thus preventing the early clogging of the karst system. Flash floods from the proximal, steep source area that is inferred by the sedimentology of the deposits would have provided periodic flushing of the karst system.

Summary and Conclusions

An unusual combination of geological and environmental factors allowed synsedimentary karst to develop in polymictic conglomerate of the Visean Hopewell Rocks Member, which is among the least susceptible types of lithologies to host karst. Abutting against an evaporitic basin as a result of rapid fault subsidence and ongoing salt expulsion in the area at the time, the coarse, proximal deposits are interpreted to have been intermittently invaded by highly alkaline groundwater during times of glacioeustatically controlled high base level, leading to their early cementation by calcite and their subsequent karstification when base level was decreasing.

These conclusions are mainly contextual and based on probable relationships drawn from the unusual tectonic and environmental settings of the succession that hosts the karst. The limited information that can be derived from the geochemistry and mineralogy of the karst infill is used as secondary evidence to suggest that alkaline groundwater was at play. They indicate that the main mineral-forming elements (Si, Al, Ca, and Na oxides) were removed in solution along discrete areas of concentrated groundwater flow, leaving behind oxides of K, Ti, Fe, and Mg, which are poorly soluble at high pH. Because many crustal rocks are only considerably soluble when the water pH is either extremely high or low, identification of paleokarst structures within such rocks can provide clues to identify occurrences of extreme environmental conditions in the geological record.

ACKNOWLEDGMENTS

This project was supported by a research grant from the Natural Sciences and Engineering Research Council of Canada. I wish to thank M. Gibling, J. Waldron, and A. McNeil for fruitful discussions; M. Préda for the X-ray diffraction analyses; X. Yang for the X-ray fluorescence analyses; and R. Corney for the making and carbon coating of thin sections.

REFERENCES CITED

Ami, H. M. 1902. Notes on some of the formations belonging to the Carboniferous System of eastern Canada. Can. Rec. Sci. 8:149–163.

Anderson, S. P.; Dietrich, W. E.; and Brimhall, G. H., Jr. 2002. Weathering profiles, mass-balance analysis, and rates of solute loss: linkages between weathering and erosion in a small, steep catchment. Geol. Soc. Am. Bull. 114:1143–1158.

Azimov, P. Y., and Bushmin, S. A. 2007. Solubility of minerals of metamorphic and metasomatic rocks in hydrothermal solutions of varying acidity: thermodynamic modeling at 400–800°C and 1–5 kbar. Geochem. Int. 45:1210–1234.

Belt, E. S. 1964. Revision of Nova Scotia middle Carboniferous units. Am. J. Sci. 262:653–673.

Blatt, H.; Middleton, G.; and Murray, R. 1980. Origin of sedimentary rocks (2nd ed.). Prentice Hall, Englewood Cliffs, NJ.

Brimhall, G. H., Jr.; Chadwick, O. A.; Lewis, C. J.; Compston, W.; Williams, I. S.; Danti, K. J.; Dietrich, W. E.; Power, M. E.; Hendricks, D.; and Bratt, J. 1992. Deformational mass transport and invasive processes in soil evolution. Science 255:695–702.

Correns, C. W. 1950. Zur Geochemie der Diagenese. 1. Das Verhalten von $CaCO_3$ und SiO_2. Geochim. Cosmochim. Acta 1:49–54.

Ford, D. C., and Williams, P. W. 2007. Karst geomorphology and hydrology (2nd ed.). Wiley, Chichester.

Giles, P. S. 1981. Major transgressive-regressive cycles in middle to late Visean rocks of Nova Scotia. N. S. Dep. Nat. Res. Mines Res. Branch Pap. ME 1981-2.

———. 2009. Orbital forcing and Mississippian sea level change: time series analysis of marine flooding events in the Visean Windsor Group of eastern Canada and implications for Gondwana glaciations. Bull. Can. Pet. Geol. 57:449–471.

Jordan, D. B., and Jones, G. L. 2005. The Powerscourt Conglomerate and its bearing on neotectonic activity in central east Ireland. Ir. J. Earth Sci. 23:47–54.

Jutras, P.; Mcleod, J.; Macrae, A.; and Utting, J. 2015. Complex interplay of fault kinematics, glacioeustastic variations and salt tectonics during deposition of upper Visean units over thick evaporites in the Cumberland Basin of eastern Canada. Basin Res., doi:10.1111/bre.12119.

Jutras, P., and Prichonnet, G. 2005. Record of Late Mississippian tectonics in the new Percé Group (Visean) of eastern Gaspésie, Quebec. Can. J. Earth Sci. 42:815–832.

Kvech, S., and Edwards, M. 2002. Solubility controls on aluminum in drinking water at relatively low and high pH. Water Res. 36:4356–4368.

Martel, A. T. 1987. The Sackville Basin of New Brunswick. *In* Beaumont, C., and Tankard, A. J., eds. Sedimentary basins and basin-forming mechanisms. Can. Soc. Pet. Geol. Mem. 12:327–335.

McCutcheon, S. R. 1981. Stratigraphy and paleogeography of the Windsor Group in Southern New Brunswick. MS thesis, Acadia University, Wolfville.

Richards, B. C. 2013. Current status of the international Carboniferous time scale. *In* Lucas, S. G.; Nelson, W. J.; DiMichele, W. A.; Spielmann, J. A.; Krainer, K.; Barrick, J. E.; Elrick, S.; and Voigt, S., eds. The Carboniferous-Permian transition. N. M. Mus. Nat. Hist. Sci. Bull. 60: 348–353.

Ryan, R. J., and Boehner, R. C. 1994. Geology of the Cumberland Basin, Cumberland, Colchester and Pictou Counties, Nova Scotia. N. S. Dep. Nat. Res. Mines Energy Branch Mem. 10.

Schaefer, C. E. G. R.; Fabris, J. D.; and Ker, J. C. 2008. Minerals in the clay fraction of Brazilian Latosols (Oxisols): a review. Clay Miner. 43:137–154.

St. Peter, C. J., and Johnson, S. C. 2009. Stratigraphy and structural history of the late Paleozoic Maritimes Basin in southeastern New Brunswick, Canada. N. B. Dep. Nat. Res. Mem. 3.

Vidal-Romani, J. R., and Vaquiero-Rodriguez, M. 2007. Types of granite cavities and associated speleothems: genesis and evolution. Nat. Conserv. 63:41–46.

Waldron, J. W. F.; Rygel, M. C.; Gibling, M. R.; and Calder, J. H. 2013. Evaporite tectonics and the late Paleozoic stratigraphic development of the Cumberland basin, Appalachians of Atlantic Canada. Geol. Soc. Am. Bull. 125:945–960.

Warren, J. K. 2006. Evaporites: sediments, resources and hydrocarbons. Berlin, Springer.

Willems, L.; Compère, P. H.; Hatert, F.; Pouclet, A; Vicat, J. P.; Ek, C.; and Boulvain, F. 2002. Karst in granitic rocks, South Cameroon: cave genesis and silica and taranakite speleothems. Terra Nova 14:355–362.